Embryological-origin-dependent differences in Hox expression in adult aorta: Role in regional phenotypic variability and regulation of NF-κB activity

Laia Trigueros-Motos[1], José M. González-Granado[1], Christine Cheung[2, †], Patricia Fernández[1, † †], Fátima Sánchez-Cabo[3], Ana Dopazo[4], Sanjay Sinha[2], Vicente Andrés[1, *]

[1] Departamento de Epidemiología, Aterotrombosis e Imagen, Centro Nacional de Investigaciones Cardiovasculares (CNIC)

[2] The Anne McLaren Laboratory for Regenerative Medicine, University of Cambridge, Cambridge. Division of Cardiovascular Medicine, University of Cambridge, Addenbrooke's Hospital, Cambridge, UK

[3] Bioinformatics Unit, CNIC

[4] Genomics Unit, CNIC

† **Current Address**: Institute of Molecular and Cell Biology, Biopolis, Proteos, Singapore

† † **Current Address**: National Cancer Institute, NIH, 41 Library Drive, Bldg. 41, B513 Bethesda, MD 20892, USA

*** Corresponding author:**
V. Andrés,
Laboratory of Molecular and Genetic Cardiovascular Pathophysiology
Departamento de Epidemiología, Aterotrombosis e Imagen
Centro Nacional de Investigaciones Cardiovasculares (CNIC)
Melchor Fernández Almagro 3, 28029 Madrid (Spain)
Phone: +34-91 453 12 00 (Ext. 1502)
Fax: +34-91 453 12 65
E-mail: vandres@cnic.es

Word count of body: 6435
Word count of abstract: 243
Total number of figures and tables: 6 Figures
Short title: Homeobox and adult vascular phenotypic variability

ABSTRACT

Objective: Different vascular beds show differing susceptibility to the development of atherosclerosis, but the molecular mechanisms underlying these differences are incompletely understood. This study aims to identify factors that contribute to the phenotypic heterogeneity of distinct regions of the adult vasculature.

Approach/Results: High-throughput mRNA profiling in adult mice reveals higher expression of the homeobox paralogous genes 6 to 10 (Hox6-10) in the athero-resistant thoracic aorta (TA) versus the athero-susceptible aortic arch (AA). Higher Hox gene expression also occurs in rat and porcine TA, and is maintained in primary smooth muscle cells isolated from TA (TA-SMCs) compared with cells from AA (AA-SMCs). This region-specific homeobox gene expression pattern is also observed in human embryonic stem cells differentiated into neuroectoderm-SMCs and paraxial mesoderm-SMCs, which give rise to AA-SMCs and TA-SMCs, respectively. We also find that, compared with AA and AA-SMCs, TA and TA-SMCs have lower activity of the pro-inflammatory and pro-atherogenic transcription factor NF-κB and lower expression of NF-κB target genes, at least in part due to HOXA9-dependent inhibition. Conversely, NF-κB inhibits HOXA9 promoter activity and mRNA expression in SMCs.

Conclusions: Our findings support a model of Hox6-10-specified positional identity in the adult vasculature that is established by embryonic cues independently of environmental factors and is conserved in different mammalian species. Differential Hox expression contributes to maintaining phenotypic differences between SMCs from athero-resistant and athero-susceptible regions, at least in part through feedback regulatory mechanisms involving inflammatory mediators, for example reciprocal inhibition between HOXA9 and NF-κB.

INTRODUCTION

Animal and human studies have conclusively established that different blood vessels and distinct segments within a given artery are heterogeneous in their susceptibility to developing vascular pathologies in response to common risk factors.[1-3] Differences in flow patterns and hemodynamic forces within the vascular system are thought to play a major role in establishing regional heterogeneity in the susceptibility to vascular disease initiation and progression.[4-6] For example, vascular regions with low shear stress or oscillatory and turbulent shear stress, such as regions of curvature and branching, are more susceptible to atherosclerotic plaque formation. In contrast, straight vessel segments with laminar blood flow are relatively resistant to atherosclerosis development. Moreover, there is evidence that, independently of hemodynamic factors, intrinsic cellular features that in part reflect distinct embryonic origins also contribute to establishing heterogeneous vascular responses to particular biological or pathological stimuli in adult organisms.[7, 8] For example, using a canine model of homograft transplantation, Haimovici and Maier found that atherosclerosis-prone abdominal aortic segments transplanted into atherosclerosis-resistant regions develop atherosclerosis, and that conversely, atherosclerosis-resistant vessels fail to develop intimal lesions when transplanted into atherosclerosis-prone positions in the abdominal aorta.[9, 10] It is also noteworthy that some regional heterogeneity of the vascular system is maintained in vitro.[7, 8] For example, cell proliferation and migration, both of which contribute to atherosclerosis development,[11, 12] are greater in primary smooth muscle cells (SMCs) derived from atherosclerosis-prone coronary artery and aortic arch than in SMCs from athero-resistant femoral arteries.[13, 14]

Previous studies demonstrated variation in susceptibility to atherosclerosis among inbred strains of wild-type mice fed an atherogenic diet, with C57BL/6J being the most susceptible.[15] Disease progression is aggravated in mice deficient for apolipoprotein E (apoE-KO), which show impaired clearing of plasma lipoproteins and develop atherosclerosis in a short time.[16] In the present study, we performed high-throughput transcriptomic studies in aorta of young C57BL/6J wild-type and apoE-KO mice fed low-fat standard chow to identify novel mediators that contribute to establishing phenotypic differences between the highly atherogenic aortic arch (AA) and the athero-resistant thoracic aorta (TA) at pre-lesional stages. We focused on genes displaying differential expression in AA compared with TA in both wild-type and apoE-KO mice, since these genes are more likely to be regulated by positional cues independently of genotype. We demonstrate that transcription factors of the homeobox gene family show significant differences in mRNA and protein expression between adult TA and AA in wild-type and apoE-KO mice. Homeobox genes encode homeodomain-containing transcription factors that are master regulators of embryonic development and specify cell fates along the anterior-posterior axis of all bilaterian embryos from a wide range of evolutionarily very distant animal species.[17-20] The class I vertebrate homeobox genes (HOX in humans and pigs, Hox in mice and rats) include 39 members organized in four paralogous clusters (Hoxa, Hoxb, Hoxc, Hoxd) that are located in different chromosomes **(see Fig.2B)**. During development, Hox genes are expressed in a temporally and spatially colinear pattern, with the most 3' members of each cluster being expressed earlier in embryonic development and predominantly in anterior regions, while the most 5' genes are activated later, mainly in posterior tissues.[17-20] We report that differences Hox gene expression between TA and AA found in the mouse are conserved in rats and pigs, and are maintained in primary adult SMCs and in developmental-origin-specific human SMCs cultured under static conditions. We also provide evidence that differences in Hoxa9 expression in distinct vessel segments contribute to establishing differential activity of the pro-atherogenic transcription factor NF-κB, which in turn represses Hoxa9 expression.

RESULTS

Global analysis of gene expression in mouse aortic arch and thoracic aorta. To identify factors involved in establishing vascular heterogeneity that may contribute to atherosclerosis development in adulthood, we performed high-throughput transcriptomic analysis of athero-susceptible AA and athero-resistant TA isolated from young wild-type and apoE-KO mice fed control chow. As expected, wild-type mice were normocholesterolemic and apoE-KO mice exhibited mild hypercholesterolemia **(Fig.1A).** Consistent with a very early stage of atherosclerosis development, atherosclerotic lesions in the aortic sinus of apoE-KO mice were absent or very incipient, as demonstrated by immunohistochemical analysis with macrophage-specific anti-Mac-3 antibody **(Fig.1B)**, and atherosclerotic lesions were completely absent from wild-type mice (data not shown). We hybridized labeled aRNA from pooled AA and TA to Agilent Whole Mouse Genome Microarrays **(Fig.1C)**. After normalization and filtering of data as described in Materials and Methods, we focused on differentially expressed genes (adjp ≤ 0.05) showing differences in expression of at least two-fold between TA and AA for at least one genotype. Using these criteria, we identified a total of 368 genes differentially expressed in TA compared with AA **(Fig.1C)**, of which 122 were differentially expressed only in apoE-KO mice (36 upregulated, 86 downregulated, **Supplemental Table II**), 27 only in wild-type mice (17 upregulated, 10 downregulated, **Supplemental Table III**), and 219 in both genotypes (82 upregulated, 137 downregulated, **Supplemental Table IV**) **(Fig.1C). Supplemental Table V** shows the functional classification of all the genes differentially expressed between TA and AA according to the Biological Process gene ontology terms (level 1) using the online software The **D**atabase for **A**nnotation, **V**isualization and **I**ntegrated **D**iscovery (**DAVID,** v6.7).

Differential regulation of class I homeobox genes in mouse aorta. We focused on genes that were differentially expressed between TA and AA in both wild-type and apoE-KO mice, since these are more likely to be regulated by positional cues independently of genotype. We noted that a subset of 11 TA-enriched genes in the Developmental Processes category were homeobox genes **(Supplemental Table V)**. Indeed, the most upregulated gene in our microarray analysis is Hoxc9, and 6 out of the 10 most upregulated transcripts in TA also correspond to Hox genes **(Supplemental Table IV)**. The magnitude of the increase in Hox expression is similar for both genotypes **(Fig.2A)**, consistent with the notion that they are truly regulated in a region-dependent manner and independently of the genotype. Our microarray studies also reveal that Hoxb8 and Hoxc8 are expressed at higher level in TA versus AA in apoE-KO mice, but not in wild-type mice **(Fig.2A)**.

Consistent with the spatial colinearity that characterizes the Hox cluster genes during embryonic development,[17-20] all the Hox genes that are expressed at higher level in mouse TA versus AA, with the sole exception of Hoxd4, belong to paralogous groups 6 to 10 of the four Hox clusters (**Fig.2B**). qPCR analysis of fresh RNA preparations (4 pools each containing 3 AAs or 3 TAs) confirmed higher expression of Hox6-10 transcripts in TA from wild-type mice (**Fig.3A, left**), including some members of these paralogous groups which were either not detected in wild-type tissue or did not pass the selection criteria in the microarray analysis. Western blot analysis of 3 independent pools of aortic tissue confirmed higher expression of Hoxa9 and Hoxc8 proteins in mouse TA compared with AA (**Fig.3B**). In contrast, expression of the 3'-most genes Hoxa1 and Hoxa2 did not differ between AA and TA **(Supplemental Fig.I).** These results show that spatial colinearity is also a characteristic of Hox gene expression in the adult mouse aorta.

To ascertain whether differential Hox expression is maintained in culture, we performed qPCR in primary SMCs isolated from mouse AA (AA-SMCs) and TA (TA-SMCs). These studies revealed higher Hox6-10 expression in TA-SMCs versus AA-SMCs, although Hoxd8 differential expression was not statistically significant (**Fig.3A, right**).

Regional differences in Hox expression in aorta are conserved in rats and pigs. In order to determine if the Hox expression pattern in the adult vasculature is conserved in mammals, we performed mRNA expression studies in aorta from rats and pigs. As in the mouse models, Hoxc8, Hoxa9 and Hoxc9 are expressed at higher level in rat TA and TA-SMCs than in AA and AA-SMCs

(**Supplemental Fig.II**). In contrast, expression of the 3'-most genes Hoxa1 and Hoxa2 is lower in rat TA and TA-SMCs (**Supplemental Fig.I**). Higher levels of HOXC8, HOXA9 and HOXC10 expression in TA compared with AA was also detected in pig (**Supplemental Fig.II**).

Human neuroectoderm-derived and paraxial mesoderm-derived smooth muscle cells exhibit differential homeobox gene expression. The vasculature is formed by SMCs from different embryological origins.[7, 8] Lineage mapping studies have shown that neural crest cells give rise to AA-SMCs whereas TA-SMCs derive from paraxial mesoderm.[7, 21] We therefore examined HOX expression in human neuroectoderm-derived SMCs (NE-SMCs) and paraxial mesoderm-derived SMCs (PM-SMCs) differentiated from pluripotent human embryonic stem cells (**Fig.4A**).[22] These in-vitro-derived cells express markers of differentiated SMCs and recapitulate the unique proliferative and secretory responses to cytokines characteristic of their in vivo aortic SMC counterparts of distinct embryonic origin.[22] In agreement with our analysis in animal models, microarray studies showed higher expression of HOXB6, C6, B7, B8, C8, A9, C9, A10 and D10 genes in human PM-SMCs than in NE-SMCs (**Fig.4B**). Higher expression of HOXC6, B7, C8, A9 and A10 in PM-SMCs versus NE-SMCs was confirmed by qPCR (**Fig.4C**). In contrast, HOXA1 was expressed at similar levels in both cell types, and HOXA2 was down-regulated in PM-SMCs (**Supplemental Fig.I**). In-vitro-derived NE-SMCs and PM-SMCs thus recapitulate the differences in HOX expression pattern observed in adult AA and TA.

Negative feedback regulation between HOXA9 and NF-κB in smooth muscle cells. Atherosclerosis is a chronic inflammatory disease,[23] and the transcription factor NF-κB plays an important role in the process of vascular inflammation.[24] Previous studies demonstrated that NF-κB is activated in the endothelium of athero-susceptible regions,[25, 26] and is downregulated by HOXA9 in human endothelial cells.[27] Consistent with these findings, our microarray studies show lower expression of the NF-κB targets E-selectin, galectin 3 and cxcl5 in the athero-resistant TA. However, it remains to be established whether HOXA9 and NF-κB are functionally related in SMCs and whether such a relationship contributes to differential expression or activity of these transcription factors in the adult vasculature. To tackle this question, we performed electrophoretic mobility shift assays (EMSA) on extracts of aortic tissue or primary SMCs. Incubation of mouse aortic extracts with a radiolabeled probe containing the consensus DNA-binding site for NF-κB generated a retarded band that was efficiently competed out with an excess of unlabeled consensus oligonucleotide, but not with an equivalent molar excess of the mutated sequence (**Fig.5A, ln.1-3**). This retarded band was supershifted upon incubation with an antibody against the NF-κB subunit p65, but not with an antibody against the unrelated protein CREB II **(Fig.5A, ln.4-5).** Similarly, incubation of rat aortic SMC extracts with the radiolabeled NF-κB consensus binding site generated a retarded band that was competed with an excess of unlabeled consensus sequence but not with equivalent amount of the mutated sequence **(Fig.5A, ln. 6-8).** This retarded band was also abrogated/supershifted using two anti-p65 antibodies but not with anti-CREB II **(Fig.5A, ln.9-11).** These results demonstrate that murine aorta and aortic SMCs exhibit NF-κB DNA-binding activity. Importantly, we found higher NF-κB DNA-binding activity in mouse AA and mouse and rat AA-SMCs than in their TA counterparts, although differences did not reach statistical significance for mouse AA and TA **(Fig.5B, Fig.5C)**. Accordingly, we observed higher expression of NF-κB targets in mouse AA and AA-SMCs than in their TA counterparts, examined by western blot analysis **(Fig.5D)** and flow cytometry **(Fig.5E).**

We next investigated whether HOXA9 regulates NF-κB activity in SMCs. For this analysis, SMCs were transiently transfected with the 5xNF-κB-luciferase reporter construct, in which luciferase expression is driven by a tandem repeat of five NF-κB binding sites. Ectopic expression of human HOXA9, but not HOXA2, significantly reduced 5xNF-κB-luciferase activity in rat aortic E19P cells and, as expected, overexpression of the NF-κB super-repressor mut IκBα[28] reduced 5xNF-κB-luciferase activity **(Fig.6A, top graph).** Similar results were obtained in mouse and rat AA-SMCs **(Fig.6A, middle and bottom graphs, respectively)**, which have higher NF-κB activity and lower Hoxa9 expression than their TA counterparts. Thus, overexpression of HOXA9 significantly inhibits NF-κB-dependent transcription in rat aorta E19P cells and AA-SMCs.

We also examined whether NF-κB can inhibit transcription driven by the human HOXA9 promoter. Activity of the HOXA9 promoter-luciferase reporter was inhibited in E19P cells by co-transfection of NF-κB/p65 or treatment with TNFα (**Fig.6B, top graph**). The inhibitory effect of TNFα was abrogated by co-transfecting mut IκBα, demonstrating the involvement of NF-κB (**Fig.6B, top graph**). Similarly, NF-κB/p65 overexpression significantly inhibited HOXA9 promoter-luciferase activity in mouse and rat TA-SMCs (**Fig.6B, middle and bottom graphs, respectively**), which have lower NF-κB activity and higher Hoxa9 expression than their AA counterparts. Moreover, transfection with NF-κB/p65 or treatment with TNFα downregulated Hoxa9 mRNA expression in rat E19P cells (**Fig.6C**).

To further examine the role of Hoxa9 in the regulation of NF-κB activity, we performed loss-of-function experiments in E19P and TA-SMCs. Cells were transiently transfected with Hoxa9-siRNA or control-siRNA and protein expression was analyzed by flow cytometry. Compared with control-siRNA, Hoxa9-siRNA reduced the levels of endogenous Hoxa9 protein without affecting β-actin expression, and this was accompanied by increased expression of the NF-κB targets Stat 5, c-myc and E-selectin (**Fig.6D**). Taken together, these results demonstrate higher NF-κB DNA-binding activity in athero-susceptible AA and AA-SMCs than in athero-resistant TA and TA-SMCs, and that HOXA9 and NF-κB inhibit each other in AA- and TA-SMCs isolated from wild-type mice and rats (**Fig.6E)**.

DISCUSSION

The main objective of the present study was to identify factors involved in establishing vascular heterogeneity that may contribute to atherosclerosis development in adulthood. Our high-throughput microarray studies were carried out in young mice fed standard chow, in which atherosclerotic lesions were either absent (wild-type) or absent/very incipient (apoE-KO). This allowed us to detect genes differentially regulated in athero-prone AA and athero-resistant TA at pre-lesional stages, which may therefore be causally related to atherosclerosis development at later phases. Although we identified genes that were differentially expressed only in wild-type mice (27 genes) or only in apoE-KO mice (127 genes), we focused on the 219 genes that were altered in AA versus TA in both wild-type and apoE-KO mice, since these are more likely to be regulated by positional cues independently of genotype. Among these genes, Hox cluster genes 6-10 are highly expressed in mouse TA compared with AA. We also demonstrate that Hox genes are highly expressed in adult rat and swine TA compared with AA. This pattern of Hox-specified positional identity in the adult vasculature of mammals is also observed in developmental origin-specific human SMCs derived in vitro from embryonic stem cells, and is maintained in mouse and rat primary SMCs isolated from adult AA and TA and cultured under static conditions. We have also shown reciprocal negative regulation between HOXA9, which is highly expressed in TA, and the pro-inflammatory and pro-atherogenic transcription factor NF-κB, which is more active in AA**.** Based on these results in tissue and SMCs obtained from wild-type mice and rats, we propose that embryonically-imprinted differential Hox expression may contribute to the establishment of distinct regional molecular signatures in the adult vasculature that are of likely importance in pathophysiological processes **(Fig.6E).**

Although our results in aortic tissue and SMC cultures are qualitatively consistent for most of the studied Hox genes (higher expression in TA and TA-SMCs versus AA and AA-SMCs), there are some dissimilarities in the size of the differences between aortic tissue and SMC cultures; for example, Hoxa10 level is ~10-fold higher in mouse TA versus AA, but ~80-fold in TA-SMC versus AA-SMC **(Fig.3A)**, and the Hoxa9 level is >60-fold higher in rat TA versus AA, but only ~8-fold higher in TA-SMC versus AA-SMC) **(Supplemental Fig.I).** These differences suggest that homeobox gene expression in SMCs might be affected by cues from other neighbouring mural cell types, which might also exhibit AA versus TA differences in Hox gene expression. It would be therefore interesting to perform in situ hybridization experiments in AA and TA to identify the cell

types expressing Hox genes, which might also reveal unknown gradients of Hox gene expression. To further explore the relationships between Hox expression and athero-susceptibility in different vascular cells, these in situ studies should also include other vessels. For example, it would be of interest to examine the athero-prone abdominal aorta, which contains SMCs of somitic-mesoderm origin, like the athero-resistant TA, and the athero-prone carotid artery, which contains SMCs from neural crest origin, like the athero-susceptible AA.[7, 8, 21]

The Hox transcription factors are known to be involved in determining positional identity and tissue specialization in the developing embryo in a wide range of evolutionarily distant animal species, including Caenorhabditis elegans, Amphioxus, Drosophila, fish, frog, chick, mouse and humans.[17-20] Comprehensive expression profiling of highly homologous Hox genes in different post-natal and adult tissues suggests a continuation of embryonic patterning;[29-31] however, the functions of Hox genes after birth remain largely unexplored and subject to speculation.[31] Previous studies have implicated a few individual Hox and non-clustered homeobox genes in physiological and pathological cardiovascular remodelling (reviewed in[32-34]). For example, Miano et al.[35] observed preferential HOXB7 and HOXC9 mRNA expression in fetal compared with adult SMCs and in rat pup versus adult SMCs, consistent with the notion that differential HOX expression may contribute to establishing phenotypic diversity in VSMCs. Moreover, Chi et al.[36] found that human SMCs isolated from different adult anatomical sites (bronchus, vein, artery, urinary tract, colon, uterus, cervix) can be clustered based solely on their pattern of expression of 63 homeobox genes, and suggested that positional information encoded in the pattern of HOX genes may play an important role in determining the distinct molecular phenotypes of SMCs from different organs. However, these authors did not compare differences in HOX gene expression between vascular SMCs obtained from different arteries, such as aorta and the coronary, pulmonary, iliac and umbilical arteries. Indeed, information on the expression of Hox genes in different regions of the adult vasculature is very scarce, with only a few studies analyzing the expression of a limited number of individual family members and their correlation with susceptibility to vascular pathologies.[25, 37-40] Endogenous gene expression studies and reporter gene analysis in transgenic mice revealed Hoxa3 and Hoxc11 expression in subsets of vascular SMCs and endothelial cells located in distinct regions of the adult vasculature that roughly corresponded to the embryonic expression domains of the two genes.[39] Higher HOXA1 and lower HOXA9 and HOXA10 expression were found in swine endothelium from athero-susceptible compared with athero-resistant vessels.[25, 37, 40] Moreover, HOXA4 expression is lower in the adult baboon abdominal aorta than in the TA and in human abdominal aortic aneurysms than in control tissue.[38] As a first step toward understanding the intrinsic phenotypic differences between arterial segments with distinct susceptibility to atherosclerosis, we performed high-throughput transcriptomic analysis of mouse athero-resistant TA and atherosclerosis-prone AA. To our knowledge, our unbiased analysis of wild-type and apoE-KO mice is the first to identify a spatially coordinated and concerted expression of all members of the Hox paralogous groups 6-10 along the mature aorta, with higher expression of Hox6-10 in TA than in AA. Importantly, we confirmed these results in TA and AA from adult rats and pigs. These findings are in agreement with the well-established notion of spatial colinearity of Hox genes during embryonic development, with the most downstream (3´) and upstream (5´) members of each cluster being expressed predominantly in anterior and posterior regions, respectively.[17-20]

The AA and TA are subject to different fluid mechanical forces generated by distinct blood flow patterns, and these forces make a central contribution to determining atherosclerosis susceptibility at least in part by establishing specific genetic regulatory programs.[4-6] Therefore differences in Hox6-10 gene expression along the aorta might be imposed by hemodynamic factors. Although we find that the differences between AA and TA observed in vivo persist in primary AA-SMCs and TA-SMCs cultured under static conditions, we cannot rule out the possibility that blood flow-dependent irreversible epigenetic changes imprinted in vivo account for differential Hox6-10 expression in cultured cells. Likewise, distinct paracrine effects caused by neighboring cells present in the vessel wall, including endothelial cells, fibroblasts, and immune cells, might impose irreversible epigenetic modifications on SMCs. This is improbable, however, given our studies using developmental origin-specific NE-SMCs and PM-SMCs derived from human embryonic stem cells, which express markers of differentiated SMCs and recapitulate key phenotypic features of AA-SMCs and TA-SMCs, respectively.[22] Although these in-vitro-derived cells have never been exposed to fluid

mechanical forces and were not co-cultured with other cell types, we found higher HOX6-10 expression in PM-SMCs than in NE-SMCs. These results support the idea that higher Hox6-10 expression in TA is caused by hard-wired embryonic programs and not post-natal environmental cues.

Differential Hox6-10 expression between the AA and TA might be a conserved mechanism that helps to explain why these vessel segments respond differently to common cardiovascular risk factors. However, demonstrating such a cause-and-effect relationship is difficult because of the involvement of multiple homeobox genes with a high degree of sequence similarity, particularly among paralogous Hox genes. Indeed, analysis of genetically-modified mice with altered Hox expression has revealed extensive functional compensation, especially among Hox genes from the same paralogous group.[17] To begin to address the functional consequences of differential Hox gene expression in adult AA and TA, we focused on Hoxa9, which is implicated in endothelial cell migration, endothelial differentiation of adult progenitor cells, and post-natal neovascularization.[41, 42] Moreover, endothelium from porcine and human athero-susceptible arteries exhibits comparatively low HOXA9 mRNA expression and high NF-κB activity.[25, 37, 40] However, we are unaware of any earlier functional study of HOXA9 in SMCs, a major component of the arterial wall that plays a key role in vascular pathophysiology. Our results demonstrate that Hoxa9 expression is lower in AA-SMCs and athero-susceptible AA than in TA-SMCs and athero-resistant TA, and this correlates with higher NF-κB activity and higher expression of NF-κB targets in AA-SMCs and AA. Moreover, in agreement with previous studies in endothelial cells,[27] our studies in SMCs show that overexpression of human HOXA9 inhibits NF-κB activity, which in turn represses reporter gene expression driven by the human HOXA9 promoter and rat Hoxa9 mRNA expression. We have also shown that inhibition of Hoxa9 in TA-SMCs downregulates the expression of NF-κB target genes. These findings suggest that reciprocal inhibition between HOXA9 and NF-κB in endothelial cells and SMCs contributes to differences in athero-suceptibility between AA and TA (**Fig.6E**). Since our functional studies were carried out with SMCs obtained from wild-type rodents, future studies will be needed to ascertain whether this model can be applied in the setting of the chronic inflammatory stress that characterizes atherosclerosis progression. Further high-throughput studies are also warranted to identify the repertoire of genes differentially regulated in AA versus TA as a result of differential Hox6-10 expression, which may shed light on the molecular mechanisms underlying the distinct response of vascular cells to cardiovascular risk factors depending on their embryonic origin.

ACKNOWLEDGEMENTS

We are grateful to colleagues who generously provided reagents (C. Shanahan for E19P cells; C. Patel for the plasmids pcDNA3.1^{+}-HOXA9, pcDNA3.1^{+}-HOXA2, p65-GFP, 5xNF-κB-luciferase and pGL3-basic HOXA9 promoter-luciferase; P. Muñoz-Canoves for mut IκBα). We also thank M. J. Andrés-Manzano for help with figure preparation, M. Torres for helpful discussions, S. Bartlett for English editing, J. Mateos, I. Longobardo and L. Cirillo for technical assistance, B. Ibáñez, J.M. García, A. García, M. Nuño, A. Macías and G. J. López for providing pig arteries, and Á. Vinué, I. Ortega and the CNIC's Animal Facility for animal care. Microarray studies were conducted by the CNIC Genomics and Bioinformatics Units.

SOURCES OF FUNDING

The author's laboratories are supported by grants from the Ministerio de Economía y Competitividad (MINECO) (SAF2010-16044), Instituto de Salud Carlos III (ISCIII) (RD/06/0014/0021, RD12/0042/0028), the Belgian Society of Cardiology (Dr. Léon Dumont Prize 2010), the European Commission (Liphos-317916), the Wellcome Trust (WT078390MA) and the Cambridge Biomedical Research Centre. CC was sponsored by the Agency for Science, Technology and Research (Singapore). JMGG received salary support from the ISCIII Miguel Servet program (CP11/00145). The CNIC is supported by MINECO and Pro-CNIC Foundation.

DISCLOSURES

None.

REFERENCES

1. VanderLaan PA, Reardon CA, Getz GS. Site specificity of atherosclerosis: Site-selective responses to atherosclerotic modulators. *Arterioscler Thromb Vasc Biol*. 2004;24:12-22
2. DeBakey ME, Glaeser DH. Patterns of atherosclerosis: Effect of risk factors on recurrence and survival-analysis of 11,890 cases with more than 25-year follow-up. *Am J Cardiol*. 2000;85:1045-1053
3. Daemen MJ, De Mey JG. Regional heterogeneity of arterial structural changes. *Hypertension*. 1995;25:464-473
4. Traub O, Berk BC. Laminar shear stress: Mechanisms by which endothelial cells transduce an atheroprotective force. *Arterioscler Thromb Vasc Biol*. 1998;18:677-685
5. Gimbrone MA, Jr., García-Cardena G. Vascular endothelium, hemodynamics, and the pathobiology of atherosclerosis. *Cardiovasc Pathol*. 2012
6. Chiu JJ, Chien S. Effects of disturbed flow on vascular endothelium: Pathophysiological basis and clinical perspectives. *Physiol Rev*. 2011;91:327-387
7. Majesky MW. Developmental basis of vascular smooth muscle diversity. *Arterioscler Thromb Vasc Biol*. 2007;27:1248-1258
8. Gittenberger-de Groot AC, DeRuiter MC, Bergwerff M, Poelmann RE. Smooth muscle cell origin and its relation to heterogeneity in development and disease. *Arterioscler Thromb Vasc Biol*. 1999;19:1589-1594
9. Haimovici H, Maier N. Experimental canine atherosclerosis in autogenous abdominal aortic grafts implanted into the jugular vein. *Atherosclerosis*. 1971;13:375-384
10. Haimovici H, Maier N. Fate of aortic homografts in canine atherosclerosis. 3. Study of fresh abdominal and thoracic aortic implants into thoracic aorta: Role of tissue susceptibility in atherogenesis. *Arch Surg*. 1964;89:961-969
11. Fuster JJ, Fernádez P, González-Navarro H, Silvestre C, Nabah YN, Andrés V. Control of cell proliferation in atherosclerosis: Insights from animal models and human studies. *Cardiovasc Res*. 2010;86:254-264
12. Andrés V. Control of vascular cell proliferation and migration by cyclin-dependent kinase signalling: New perspectives and therapeutic potential. *Cardiovasc Res*. 2004;63:11-21
13. Nishiguchi F, Fukui R, Hoshiga M, Negoro N, Ii M, Nakakohji T, Kohbayashi E, Ishihara T, Hanafusa T. Different migratory and proliferative properties of smooth muscle cells of coronary and femoral artery. *Atherosclerosis*. 2003;171:39-47
14. Castro C, Díez-Juan A, Cortés MJ, Andrés V. Distinct regulation of mitogen-activated protein kinases and $p27^{kip1}$ in smooth muscle cells from different vascular beds. A potential role in establishing regional phenotypic variance. *J Biol Chem*. 2003;278:4482-4490
15. Paigen B, Morrow A, Brandon C, Mitchell D, Holmes P. Variation in susceptibility to atherosclerosis among inbred strains of mice. *Atherosclerosis*. 1985;57:65-73
16. Meir KS, Leitersdorf E. Atherosclerosis in the apolipoprotein-E-deficient mouse: A decade of progress. *Arterioscler Thromb Vasc Biol*. 2004;24:1006-1014
17. Maconochie M, Nonchev S, Morrison A, Krumlauf R. Paralogous Hox genes: Function and regulation. *Annu Rev Genet*. 1996;30:529-556
18. Krumlauf R. Hox genes in vertebrate development. *Cell*. 1994;78:191-201
19. Kmita M, Duboule D. Organizing axes in time and space; 25 years of colinear tinkering. *Science*. 2003;301:331-333
20. McGinnis W, Krumlauf R. Homeobox genes and axial patterning. *Cell*. 1992;68:283-302
21. Jiang X, Rowitch DH, Soriano P, McMahon AP, Sucov HM. Fate of the mammalian cardiac neural crest. *Development*. 2000;127:1607-1616
22. Cheung C, Bernardo AS, Trotter MW, Pedersen RA, Sinha S. Generation of human vascular smooth muscle subtypes provides insight into embryological origin-dependent disease susceptibility. *Nat Biotechnol*. 2012;30:165-173
23. Libby P, Ridker PM, Hansson GK. Progress and challenges in translating the biology of atherosclerosis. *Nature*. 2011;473:317-325
24. Brasier AR. The nuclear factor-kappab-interleukin-6 signalling pathway mediating vascular inflammation. *Cardiovasc Res*. 2010;86:211-218

25. Fang Y, Shi C, Manduchi E, Civelek M, Davies PF. MicroRNA-10a regulation of proinflammatory phenotype in athero-susceptible endothelium in vivo and in vitro. *Proc Natl Acad Sci USA*. 2010;107:13450-13455
26. Iiyama K, Hajra L, Iiyama M, Li H, DiChiara M, Medoff BD, Cybulsky MI. Patterns of vascular cell adhesion molecule-1 and intercellular adhesion molecule-1 expression in rabbit and mouse atherosclerotic lesions and at sites predisposed to lesion formation. *Circ Res*. 1999;85:199-207
27. Trivedi CM, Patel RC, Patel CV. Homeobox gene HOXA9 inhibits nuclear factor-kappa B dependent activation of endothelium. *Atherosclerosis*. 2007;195:e50-60
28. Hayden MS, Ghosh S. Signaling to NF-kappaB. *Genes Dev*. 2004;18:2195-2224
29. Takahashi Y, Hamada J, Murakawa K, Takada M, Tada M, Nogami I, Hayashi N, Nakamori S, Monden M, Miyamoto M, Katoh H, Moriuchi T. Expression profiles of 39 HOX genes in normal human adult organs and anaplastic thyroid cancer cell lines by quantitative real-time RT-PCR system. *Exp Cell Res*. 2004;293:144-153
30. Yamamoto M, Takai D, Yamamoto F, Yamamoto F. Comprehensive expression profiling of highly homologous 39 HOX genes in 26 different human adult tissues by the modified systematic multiplex RT-PCR method reveals tissue-specific expression pattern that suggests an important role of chromosomal structure in the regulation of hox gene expression in adult tissues. *Gene Expr*. 2003;11:199-210
31. Morgan R. Hox genes: A continuation of embryonic patterning? *Trends Genet*. 2006;22:67-69
32. Cantile M, Schiavo G, Terracciano L, Cillo C. Homeobox genes in normal and abnormal vasculogenesis. *Nutr Metab Cardiovasc Dis*. 2008;18:651-658
33. Gorski DH, Walsh K. Control of vascular cell differentiation by homeobox transcription factors. *Trends Cardiovasc Med*. 2003;13:213-220
34. Gorski DH, Walsh K. The role of homeobox genes in vascular remodeling and angiogenesis. *Circ Res*. 2000;87:865-872
35. Miano JM, Firulli AB, Olson EN, Hara P, Giachelli CM, Schwartz SM. Restricted expression of homeobox genes distinguishes fetal from adult human smooth muscle cells. *Proc Natl Acad Sci USA*. 1996;93:900-905
36. Chi JT, Rodriguez EH, Wang Z, Nuyten DS, Mukherjee S, van de Rijn M, van de Vijver MJ, Hastie T, Brown PO. Gene expression programs of human smooth muscle cells: Tissue-specific differentiation and prognostic significance in breast cancers. *PLoS Genet*. 2007;3:1770-1784
37. Burridge KA, Friedman MH. Environment and vascular bed origin influence differences in endothelial transcriptional profiles of coronary and iliac arteries. *Am J Physiol Heart Circ Physiol*. 2010;299:H837-846
38. Lillvis JH, Erdman R, Schworer CM, Golden A, Derr K, Gatalica Z, Cox LA, Shen J, Vander Heide RS, Lenk GM, Hlavaty L, Li L, Elmore JR, Franklin DP, Gray JL, Garvin RP, Carey DJ, Lancaster WD, Tromp G, Kuivaniemi H. Regional expression of HOXA4 along the aorta and its potential role in human abdominal aortic aneurysms. *BMC Physiol*. 2011;11:9
39. Pruett ND, Visconti RP, Jacobs DF, Scholz D, McQuinn T, Sundberg JP, Awgulewitsch A. Evidence for Hox-specified positional identities in adult vasculature. *BMC Dev Biol*. 2008;8:93
40. Zhang J, Burridge KA, Friedman MH. In vivo differences between endothelial transcriptional profiles of coronary and iliac arteries revealed by microarray analysis. *Am J Physiol Heart Circ Physiol*. 2008;295:H1556-1561
41. Bruhl T, Urbich C, Aicher D, Acker-Palmer A, Zeiher AM, Dimmeler S. Homeobox a9 transcriptionally regulates the EphB4 receptor to modulate endothelial cell migration and tube formation. *Circ Res*. 2004;94:743-751
42. Rossig L, Urbich C, Bruhl T, Dernbach E, Heeschen C, Chavakis E, Sasaki K, Aicher D, Diehl F, Seeger F, Potente M, Aicher A, Zanetta L, Dejana E, Zeiher AM, Dimmeler S. Histone deacetylase activity is essential for the expression of HoxA9 and for endothelial commitment of progenitor cells. *J Exp Med*. 2005;201:1825-1835

SIGNIFICANCE

Different blood vessels and distinct segments within a given artery are heterogeneous in their susceptibility to developing vascular pathologies in response to common risk factors, but the molecular mechanisms underlying these differences are incompletely understood. Here, we show that homeobox cluster genes 6-10 are highly expressed in mouse athero-resistant thoracic aorta (TA) compared with athero-pone aortic arch (AA). This pattern of Hox-specified positional identity is maintained in adult rat and swine TA compared with AA, in mouse and rat primary smooth muscle cells (SMCs) isolated from adult AA and TA, and in developmental origin-specific human SMCs derived in vitro from embryonic stem cells and cultured under static conditions. We also show that differential Hox expression contributes to maintaining phenotypic differences between SMCs from athero-resistant and athero-susceptible regions, at least in part through feedback regulatory mechanisms involving inflammatory mediators, for example reciprocal inhibition between HOXA9 and NF-κB.

FIGURE LEGENDS

Figure 1. Rationale and design of high-throughput analysis of atherosclerosis-related gene expression in mouse aorta. Three-month-old wild-type and apoE-KO mice were fed low-fat standard chow. **(A)** Total plasma cholesterol (n=6 mice per genotype). **(B)** Representative images of macrophage-specific anti-Mac3 immunostaining showing incipient atherosclerotic lesions in aortic sinus of apoE-KO mice (brown staining). **(C)** AA and TA were extracted from 12 mice of each genotype, and tissue was pooled to isolate total RNA for microarray studies. Using the criteria described in Material and Methods, 122 transcripts exhibited differential regulation between TA and AA only in apoE-KO mice **(Supplemental Table II),** 27 only in wild-type mice **(Supplemental Table III),** and 219 in mice of both genotypes **(Supplemental Table IV).**

Figure 2. Homeobox gene expression in mouse aorta. (A) Microarray studies revealed higher level of expression of thirteen homeobox genes in TA versus AA (11 in both genotypes, and Hoxc8 and Hoxb8 only in apoE-KO mice). **(B)** Representation of the four homeobox clusters (a-d) and individual Hox genes (1-13), showing members that are expressed at similar levels in AA and TA (white boxes) or upregulated (grey boxes) in TA versus AA.

Figure 3. Homeobox expression in mouse aortic tissue and primary SMCs. Three-month-old wild-type mice fed standard chow were sacrificed, and total RNA or protein was isolated from aortic tissue (pools of 3 AAs or TAs) or primary SMCs (established in culture from pools of 5 AAs or TAs). **(A)** Hox gene expression quantified by qPCR using 18S as an internal control. Results are presented in arbitrary units normalized to expression in AA (=1). Data are means±SEM of 4 independent extractions for mouse aortic tissue and 5 independent extractions for mouse SMCs, measured in triplicate. *: p<0.05; **: p< 0.01; ***: p<0.001. **(B)** Hoxa9 and Hoxc8 protein expression in lysates from 3 independent pools analyzed by Western blot. GAPDH was used as loading control.

Figure 4. Homeobox gene expression in in-vitro-derived human neuroectoderm- and paraxial-mesoderm-derived SMCs. (A) Scheme of *in vitro* derivation of NE-SMCs and PM-SMCs from human embryonic stem cells (hEPSCs). **(B)** HOX genes upregulated in PM-SMCs versus NE-SMCs, as revealed by microarray analysis. **(C)** qPCR analysis of HOX gene expression. Results are presented in arbitrary units normalized to NE-SMCs (mean±SEM, *n*=3). *: p<0.05; **: p< 0.01; ***: p<0.001.

Figure 5. NF-κB DNA-binding activity and target gene expression are higher in aortic arch and AA-SMCs compared with thoracic aorta and TA-SMCs. (A-C) EMSA using cell lysates and a radiolabeled oligonucleotide containing the NF-κB consensus DNA-binding site. Representative autoradiographs are shown and quantitative data in **B** and **C** are means±SEM of the indicated number of independent experiments. In the EMSA of each panel all binding reactions were run in the same gel and exposed to the same X Ray film. Cell lysates in **A** were prepared from mouse TA **(left)** and TNFα-treated rat primary TA-SMCs **(right).** For competition assays, binding reactions included a 100-fold excess of unlabeled NF-κB consensus oligonucleotide or a mutant sequence that disrupts NF-κB binding. For supershift experiments, antibodies against p65 (1: sc-372; 2: sc-109) or CREBII (negative control) were added to binding reactions. Cell lysates in **B** and **C** were prepared from AA and TA, or from AA-SMCs and TA-SMCs isolated from wild-type mice or rat, as indicated. The autoradiographs only show the retarded nucleo-protein complexes. *: p<0.05; **: p< 0.01. **(D)** Western blot analysis of mouse AA and TA. **(E)** Protein expression in AA-SMCs and TA-SMCs analyzed by flow cytometry.

Figure 6. HOXA9 and NF-κB inhibit each other in SMCs. Experiments were performed with rat embryonic aortic E19P cells, and primary mouse or rat AA- or TA-SMCs, as indicated. **(A)** Cells were transfected with a luciferase reporter gene containing a tandem repeat of five NF-κB binding sites (5xNF-κB-luciferase) plus pRL-TK renilla as a control for transfection efficiency. When indicated, cells were co-transfected with HOXA9 (pcDNA3.1^{+}-HOXA9), HOXA2 (pcDNA3.1^{+}-

HOXA2) or mut IκBα (IκBα S32/36A, NF-κB super-repressor). One day after transfection, cells were lysed and luciferase activity measured. Data are means±SEM of 4 to 7 independent experiments. **(B)** Cells were transfected with pGL3 basic-HOXA9 promoter-luciferase reporter plasmid plus pRL-TK renilla. When indicated, cells were co-transfected with mut IκBα or p65-GFP (subunit of NF-κB complex), and/or treated with TNFα (10 ng/ml during the last 4 hrs). Luciferase activity was measured after 24h. Data are means±SEM of 3 to 6 independent experiments. **(C)** E19P cells were untreated, exposed to TNFα (10 ng/ml, 4 hrs), or transiently transfected with p65-GFP, and total RNA was isolated for qPCR to quantify Hoxa9 expression using 18S as an endogenous control. Results are means±SEM of 4 independent experiments measured in triplicate (arbitrary units normalized to control cells). **(D)** Cells were transiently transfected with Hoxa9-siRNA or control-siRNA. Transfected cells were detached and levels of the indicated proteins were measured by flow cytometry. **(E)** Proposed model for the reciprocal modulation of NF-κB and HOXA9 in the adult aorta. *: $p<0.05$; **: $p< 0.01$; ***: $p<0.001$.

Figure 1

A

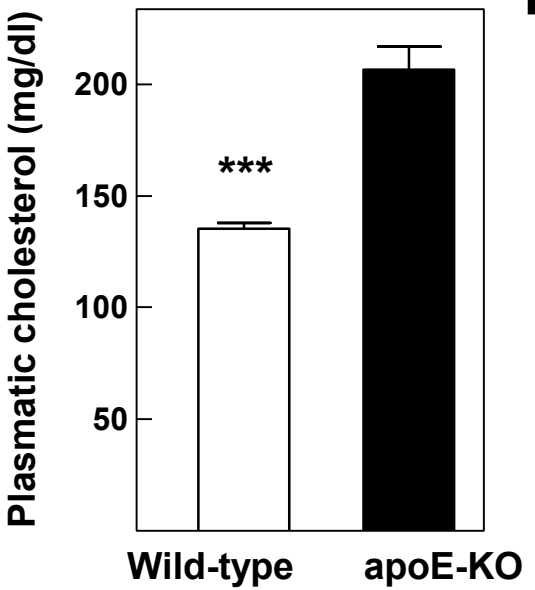

B

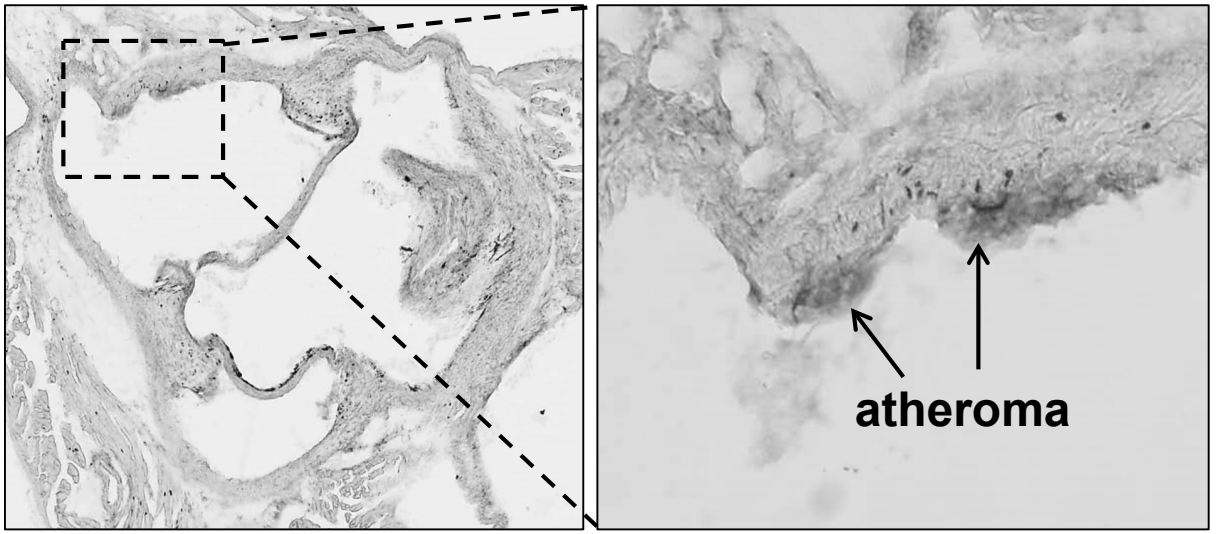

C

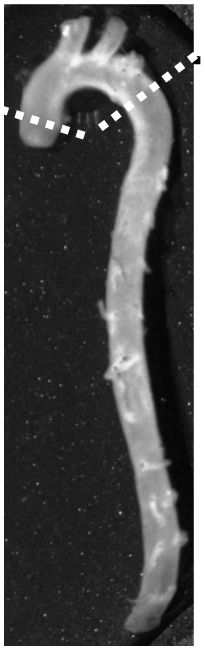

Aortic arch (AA) → 4 pools (3 AA/pool)

Thoracic aorta (TA) → 4 pools (3 TA/pool)

Agilent™ Whole Mouse Genome Microarrays (41000 transcripts) → 368 genes differentially regulated TA versus AA

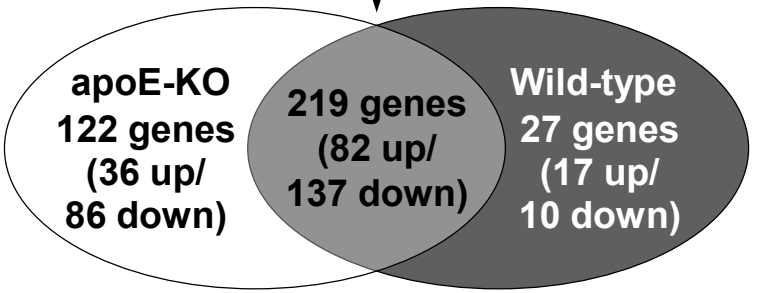

Figure 2

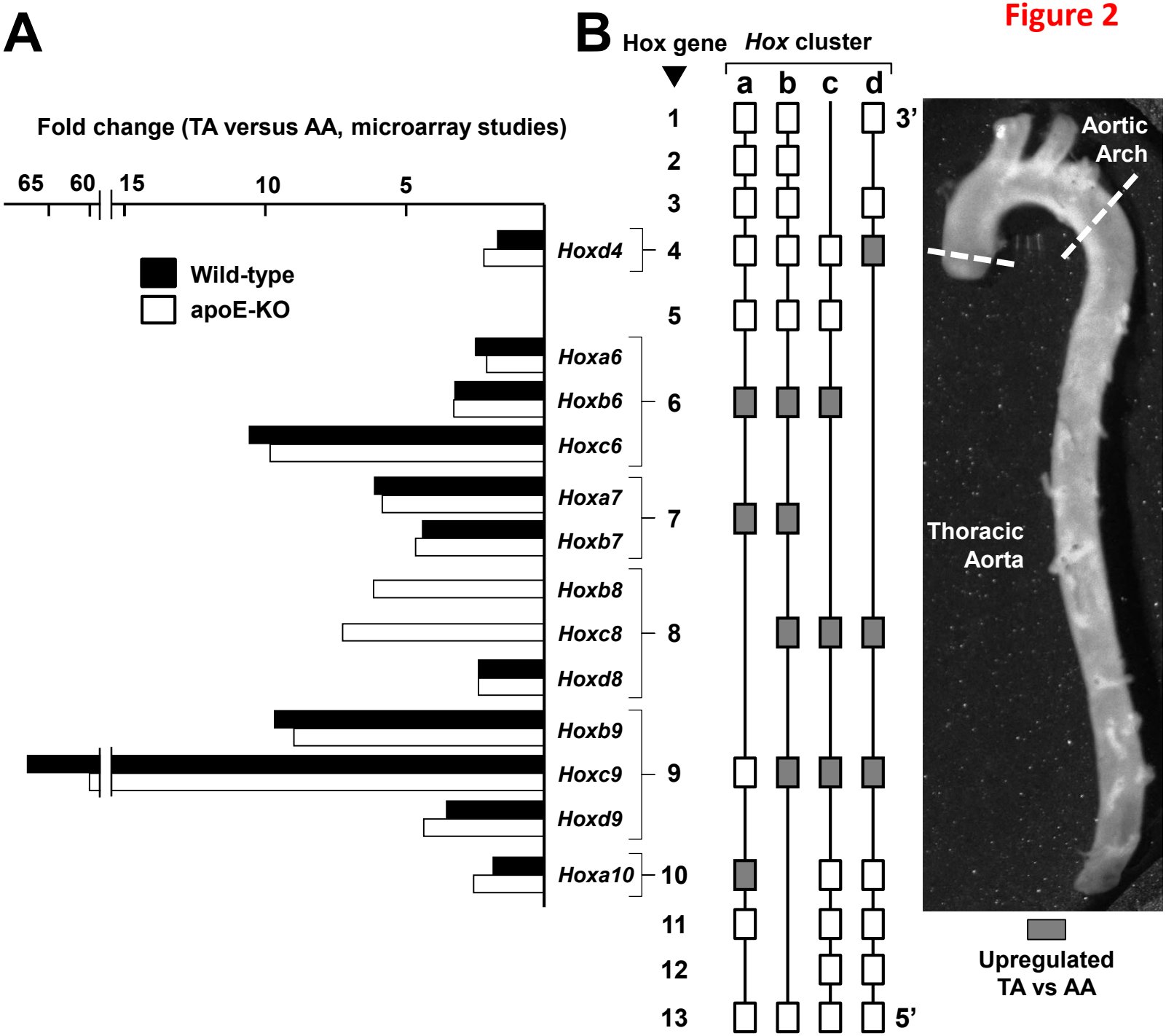
A
Fold change (TA versus AA, microarray studies)
65
60
15
10
5
Wild-type
apoE-KO
Hoxd4
Hoxa6
Hoxb6
Hoxc6
Hoxa7
Hoxb7
Hoxb8
Hoxc8
Hoxd8
Hoxb9
Hoxc9
Hoxd9
Hoxa10
B
Hox gene
Hox cluster
a
b
c
d
1
2
3
4
5
6
7
8
9
10
11
12
13
3'
5'
Aortic Arch
Thoracic Aorta
Upregulated TA vs AA

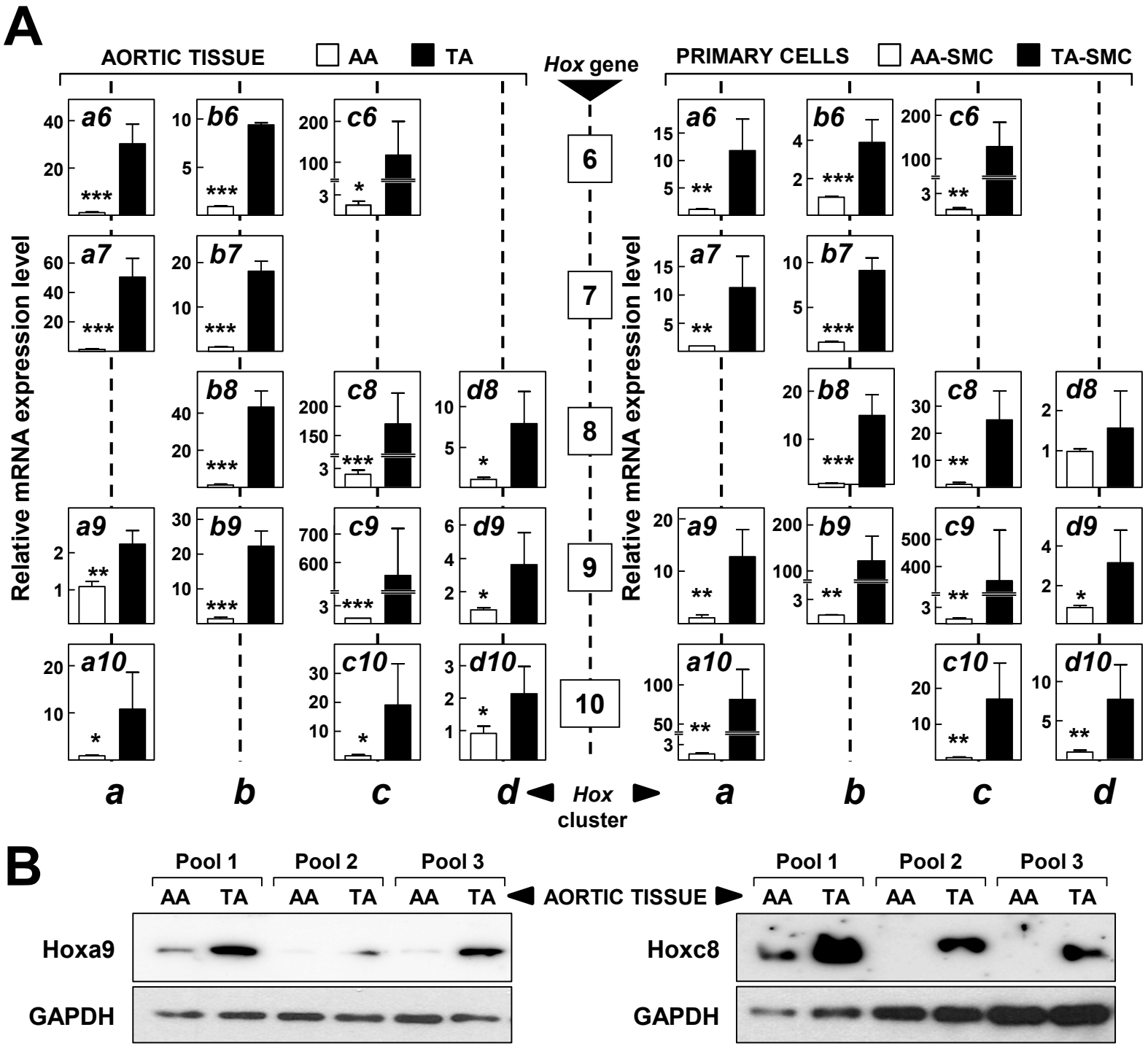
A
AORTIC TISSUE
AA
TA
Hox gene
PRIMARY CELLS
AA-SMC
TA-SMC
Relative mRNA expression level
a6
b6
c6
a7
b7
b8
c8
d8
a9
b9
c9
d9
a10
c10
d10
6
7
8
9
10
a
b
c
d
Hox cluster
B
Pool 1
Pool 2
Pool 3
AA
TA
AORTIC TISSUE
Hoxa9
GAPDH
Hoxc8
GAPDH

Figure 4

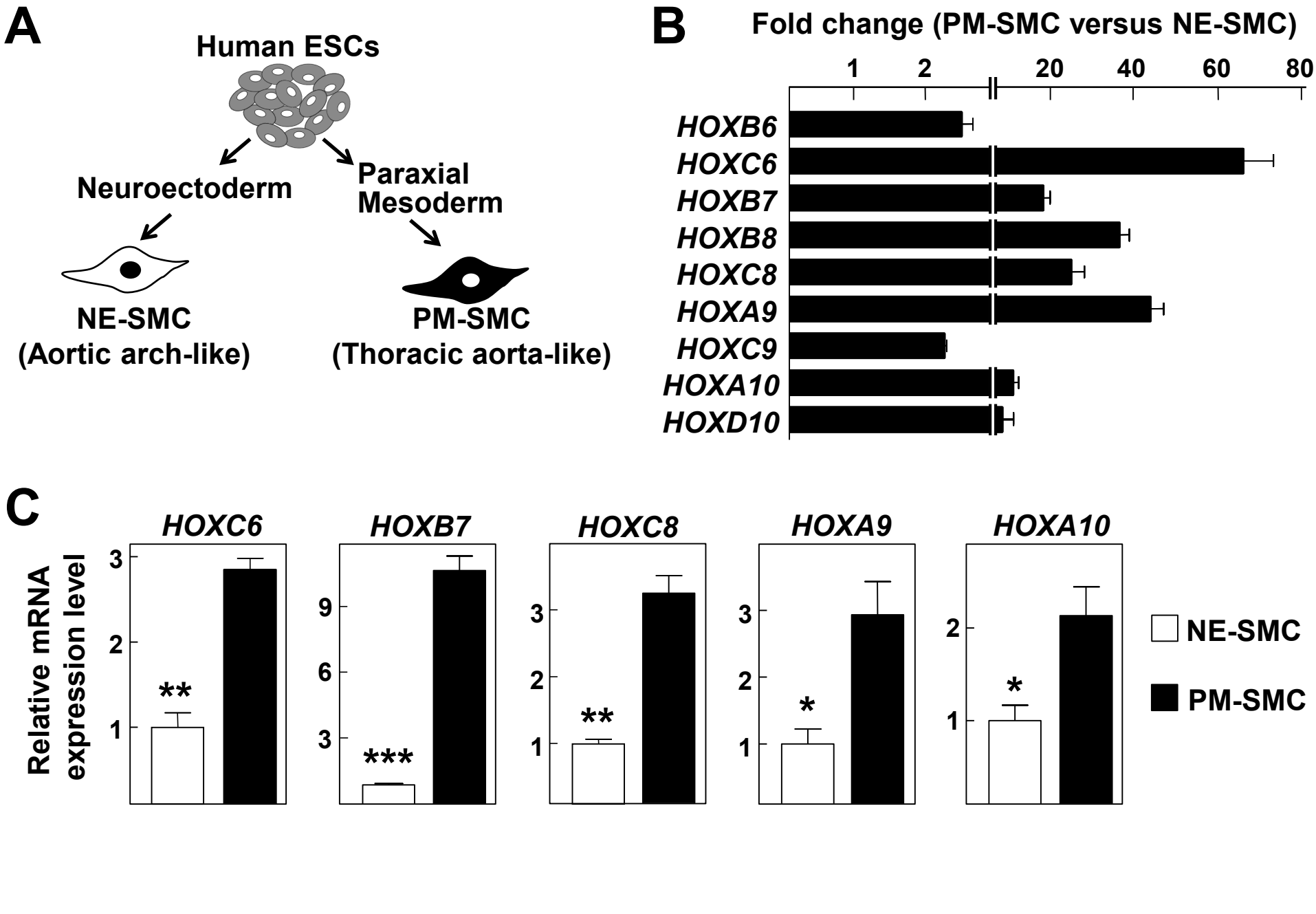
A
Human ESCs
Neuroectoderm
Paraxial Mesoderm
NE-SMC
(Aortic arch-like)
PM-SMC
(Thoracic aorta-like)
B
Fold change (PM-SMC versus NE-SMC)
1
2
20
40
60
80
HOXB6
HOXC6
HOXB7
HOXB8
HOXC8
HOXA9
HOXC9
HOXA10
HOXD10
C
HOXC6
HOXB7
HOXC8
HOXA9
HOXA10
Relative mRNA expression level
**
***
**
*
*
NE-SMC
PM-SMC

Figure 5

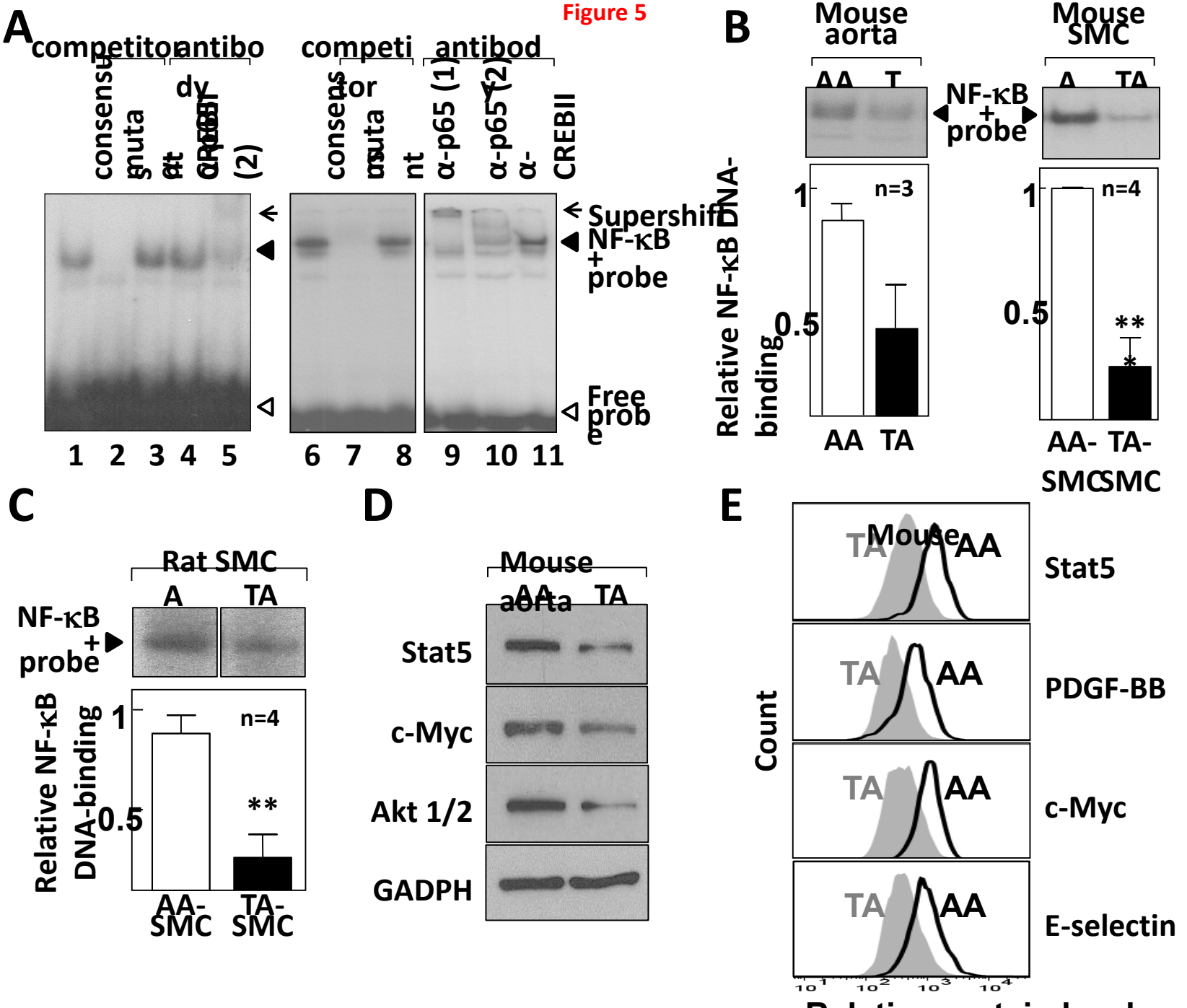
A
competitor
antibody
consensus
mutant
dy
α-p65 (1)
α-p65 (2)
α-CREBII
Supershift
NF-κB + probe
Free probe
1 2 3 4 5 6 7 8 9 10 11
B
Mouse aorta
Mouse SMC
AA
TA
NF-κB + probe
Relative NF-κB DNA-binding
n=3
n=4
1
0.5
**
*
AA
TA
AA-SMC
TA-SMC
C
Rat SMC
A
TA
NF-κB + probe
Relative NF-κB DNA-binding
n=4
**
AA-SMC
TA-SMC
D
Mouse aorta
AA
TA
Stat5
c-Myc
Akt 1/2
GADPH
E
Mouse
TA
AA
Stat5
PDGF-BB
c-Myc
E-selectin
Count
Relative protein level

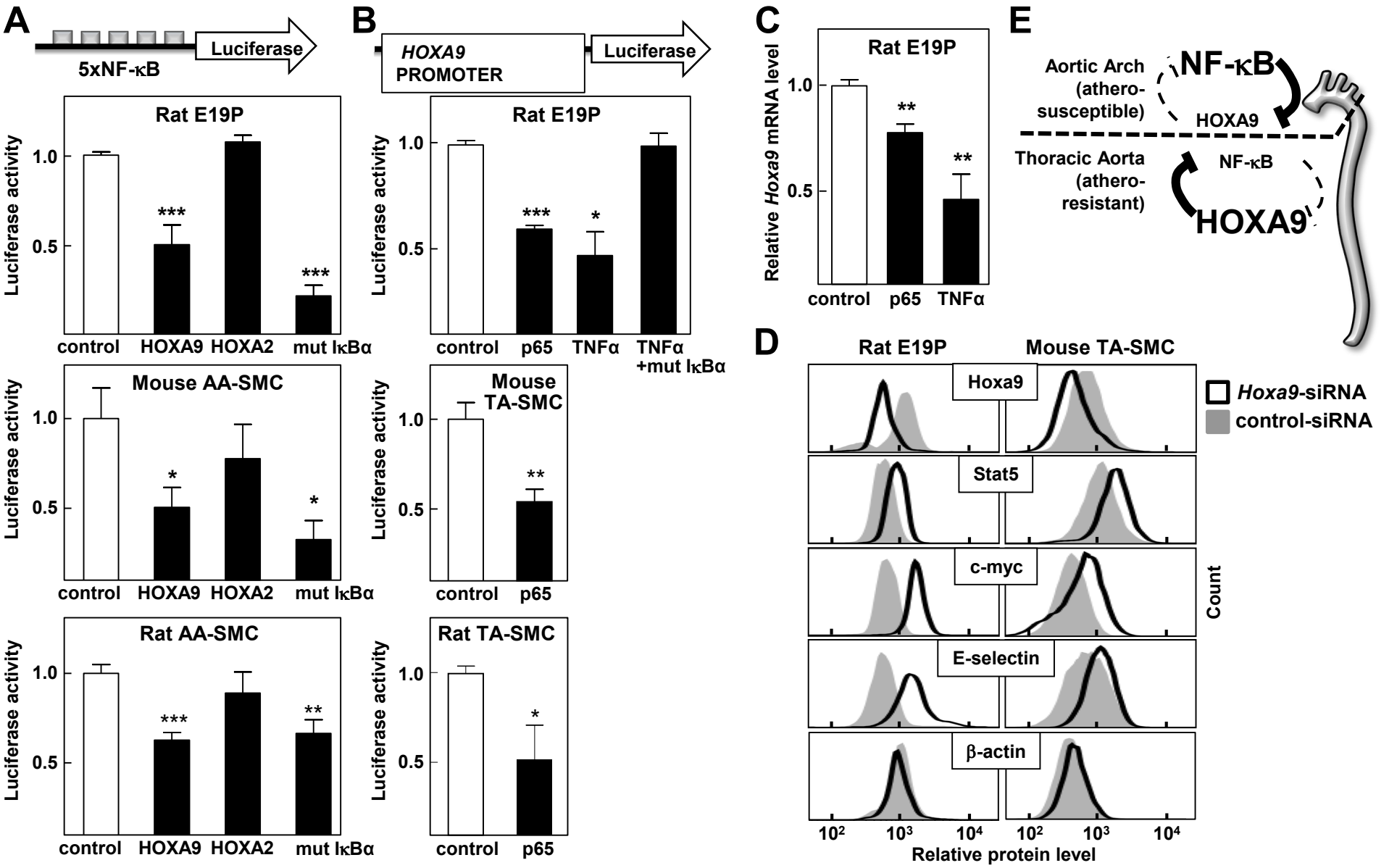
A
5xNF-κB
Luciferase
Rat E19P
Luciferase activity
control
HOXA9
HOXA2
mut IκBα
Mouse AA-SMC
Rat AA-SMC
B
HOXA9
PROMOTER
Luciferase
Rat E19P
control
p65
TNFα
TNFα
+mut IκBα
Mouse
TA-SMC
Rat TA-SMC
C
Rat E19P
Relative Hoxa9 mRNA level
control
p65
TNFα
E
Aortic Arch
(athero-
susceptible)
NF-κB
HOXA9
Thoracic Aorta
(athero-
resistant)
NF-κB
HOXA9
D
Rat E19P
Mouse TA-SMC
Hoxa9
Stat5
c-myc
E-selectin
β-actin
Hoxa9-siRNA
control-siRNA
Count
Relative protein level

MATERIALS AND METHODS

Animals. Male apolipoprotein E-null mice (apoE-KO) and wild-type mice (both C57BL/6J genetic background, Charles River Laboratories, Wilmington, Massachusetts, USA) were maintained on a low-fat standard diet (2.8% fat, Panlab, Barcelona, Spain) and were sacrificed at 3 months of age. Male Wistar rats (200-400 g, Charles River Laboratories) were sacrificed at 3 to 5 months of age. Castrated male Large-White pigs (bred on the CNIC's farm) were sacrificed at 3 to 4.5 months of age. All animal procedures conformed to Directive 2010/63EU and Recommendation 2007/526/EC regarding the protection of animals used for experimental and other scientific purposes, enforced in Spanish law under Real Decreto 1201/2005.

Microarray studies. Twelve mice of each genotype were sacrificed to isolate the AA and the TA. The aorta was removed, placed on a Petri dish containing ice-cold PBS and cleaned of surrounding fat and non-vascular tissue under a stereo microscope (Olympus SZX10, Olympus Iberia, Barcelona, Spain). Further dissection yielded the AA (from ~3 mm above the aortic root to ~2 mm past the left subclavian artery) and TA (from ~2 mm past the left subclavian artery to the diaphragm insertion) (Fig.1C). Four pools each containing 3 AAs or 3 TAs were processed for total RNA isolation using Qiazol and the miRNeasy Mini kit (Fig.1C). RNA concentration and purity were assessed from the A260nm/A280nm ratio, and integrity was verified by separation on ethidium bromide-stained 1% agarose gels. RNA was amplified and labeled using the One-Color Microarray-Based Gene Expression Analysis Protocol (Agilent Technologies, Palo Alto, CA, USA). Samples were hybridized to a Mouse Whole Genome Oligo Microarray (4x44K; G4122F, Agilent Technologies). Cyanine-3-labeled aRNAs (1.65 µg) were hybridized for 17 h in a final concentration of 1x GEx Hybridization Buffer HI-RPM (Agilent Technologies) at 65ºC in an Agilent hybridization oven (G2545A, Agilent Technologies) set to 10 rpm. Arrays were washed and dried according to the manufacturer's instructions (One-Color Microarray-Based Gene Expression Analysis, Agilent Technologies), and were scanned at 5mm resolution on an Agilent DNA Microarray Scanner (G2565BA, Agilent Technologies) using the default settings for 4x44k format one-color arrays. Images generated by the scanner were analyzed using Feature Extraction software v10.1.1.1 (Agilent Technologies). Data were normalized using the quantiles method. Two arrays that were identified as statistical outliers by the array QualityMetrics Bioconductor package were excluded from further analysis. From the original set of probes only those with a good flag and with a signal above the 20% overall array signal in at least three samples were subjected to statistical analysis. Probes showing no change (cv<25%) across all samples were also excluded from the analysis (13597 probes remaining). To detect genes differentially expressed between different conditions, we used a mixed effects model as implemented in the Limma Bioconductor package. The fixed effects were the genotype (apoE-KO/wild-type) and the region of the aorta (AA versus TA), and the mouse pool was considered a random effect. Changes were considered significant at an adjusted Benjamini-Hochberg p-value ≤ 0.05.

The Illumina HumanHT-12 v4 BeadArray was used to acquire genome-wide expression data from neuroectoderm-derived and paraxial mesoderm-derived smooth muscle cells (NE-SMCs and PM-SMCs, respectively). Data were processed as previously described.[1] Data are available from the ArrayExpress microarray data repository under the accession number E-MTAB-781.

Plasma cholesterol. Mice were fasted overnight and blood was withdrawn from the cheek. Plasma cholesterol levels were measured using an enzymatic procedure (WAKO, St. Louis, Missouri, USA).

Cell culture. Cells were maintained at 37ºC and 5% CO_2 in Dulbecco's Modified Minimal Essential Medium (DMEM) (Sigma, St. Louis, Missouri, USA) supplemented with 10% heat-inactivated fetal bovine serum (FBS, Sigma), 1% glutamine and 1% penicillin/streptomycin.

When indicated, cells were treated for 4 h with recombinant murine tumor necrosis factor α (TNF-α, 10 ng/ml, ref. 315-01A, Peprotech EC Ltd, London, UK).

The rat embryonic aorta cell line E19P was kindly provided by C. Shanahan (King's College London, UK). Mouse primary SMCs were isolated from a pool of 5 TAs or 5 AAs harvested from 3-month-old wild-type mice after 2 digestions in HBSS/fungizone medium. Briefly, the mouse aorta was first digested with type II collagenase (175 U/ml) (ref. 4176, Worthington Biochemical Corp., Lakewood, New Jersey, USA) to remove the adventitia and SMC suspensions were obtained after a second digestion with type II collagenase (175 U/ml) and type I elastase (4.7 U/ml) (ref. 45124, Sigma). For the preparation of primary rat SMCs, rat aortas were harvested and first digested with type II collagenase (590 U/ml) (ref. 4176, Worthington) in DMEM for 20 minutes at 37ºC and the adventitia was completely removed. Tissue was then cut in rings, maintained with agitation for 2h at 37ºC, and cells were plated in 6-well dishes. Mouse and rat SMCs were initially cultured in DMEM with 20% FBS and 1% fungizone/penicillin/streptomycin/glutamine, and afterwards as described above. Mouse and rat primary cells from passages 4 to 10 were used for experiments. The identity of AA and TA SMCs was confirmed by immunocytochemistry with a cyanine-3-conjugated anti-smooth-muscle-α-actin antibody (1/200 dilution) (clone 1A4, c-6198, Sigma).[2]

Human embryonic stem cells (line H9, WiCell, Madison, WI, USA, passages 65-85) were cultured and differentiated into neuroectoderm-derived SMCs (NE-SMC) and paraxial mesoderm-derived SMCs (PM-SMC) under chemically-defined conditions as previously described.[1]

Mac-3 immunostaining. Mice were sacrificed and their heart and aorta were removed after in situ perfusion with PBS. For Mac-3 immunostaining, the protion of the heart containing the aortic sinus was fixed with freshly prepared 4% paraformaldehyde/PBS overnight at 4°C. After fixation, the tissue was paraffin-embedded and 3-µm cross-sections were prepared for immunostaining with rat monoclonal anti-Mac3 antibody (1/200 dilution, clone M3/84, sc-19991, Santa Cruz Biotechnology, Santa Cruz, California, USA), followed by incubation with biotin-conjugated goat anti-rat secondary antibody (1/300 dilution, sc-2041, Santa Cruz Biotechnology), and streptavidin-HRP (TS-060-HR, Lab Vision Corporation, Fremont, California, USA). Immunocomplexes were detected with DAB substrate (BUF021A, AbD Serotec, Kidlington, UK) and specimens were counterstained with hematoxylin.

Quantitative real-time polymerase chain reaction (qPCR). Animals were sacrificed to isolate total RNA from aortic tissue (for mice, 4 pools of 3 AAs or TAs different from those used for microarray studies) or primary SMCs (for mice, pools were prepared from 5 AA or TA). Tissue disruption was performed in Qiazol Lysis Reagent using 5mm-diameter stainless steel beads and a Tissue-Lyser LT (all from Qiagen, Valencia, California, USA). The Tissue-Lyser LT adapter was precooled and used with 10 cycles of 3 minutes at 50 Hz. Total RNA was recovered from the aqueous phase and final isolation of RNA was perfomed using the miRNeasy Mini kit according to the manufacturer's instructions (Qiagen). RNA concentration and purity were assessed from the A260nm/A280nm ratio. cDNA was generated from RNA (0.5-1 μg) using random hexamers, RNase Inhibitor and the High Capacity cDNA Reverse Transcription Kit (Applied Biosystems, Foster City, California, USA). qPCR was performed with the ABI PRISM 7900HT Sequence Detection System using PCR Power SYBR Green PCR Master Mix (both from Applied Biosystems). Total RNA from human NE-SMCs and PM-SMCs was extracted with RNeasy Mini Kit (Qiagen) and cDNA was prepared with the Maxima First Strand cDNA Synthesis Kit (Fermentas, St. Leon-Rot, Germany). qPCR was performed with the 7500 Fast Real-time PCR System using SYBR Green PCR Master Mix (Applied Biosystems). Reactions were performed in technical duplicates or triplicates using the specific primers shown in Supplemental Table I. Relative quantification of gene expression was performed with the internal control housekeeping genes ribosomal 18S (for mouse and rat), glyceraldehyde-3-phosphate

dehydrogenase (for pig), or porphobilinogen deaminase (for human cells). qPCR results were analyzed by the comparative Ct method.

Antibodies. Anti-Stat 5 (sc-835), anti-Akt1/2 (sc-1619), anti-PDGF-B (sc-74494), anti-β-Actin (sc-130657), anti NFκB p65 (sc-109) and anti-HoxA9 (sc-17155) were from Santa Cruz Biotech.; anti-Myc (06-340) was from Upstate; anti-HOXC8 (ab86236) was from Abcam and PE conjugated anti-E-selectin (553751) was from BD bioscience.

Immunoblotting. Whole lysates from aorta segments or vascular SMC were subjected to SDS-PAGE, and proteins were transferred to PVDF membranes and probed with the indicated antibodies in Tris-buffered saline–Tween 20. Bound antibodies were incubated with horseradish peroxidase secondary antibodies and membranes were developed by enhanced chemiluminescence with Super-Signal West Pico or Femto chemiluminescent substrate (Pierce Chemical).

Electrophoretic mobility shift assay (EMSA). Double-stranded oligonucleotides containing the consensus DNA-binding site for nuclear factor-κB (NF-κB) (5'-AGTTGAGGGGACTTTCCCAGG-3', NF-κB binding site underlined) were labeled with [^{32}P]dATP (Perkin Elmer, Waltham, Massachusetts, USA) using polynucleotide kinase (New England Biolabs, Ipswich, Massachusetts, USA) and purified on a Sephadex G-50 column. Total protein extracts (aortic tissue: 15 µg; SMCs: 2 µg) were pre-incubated with 20 mM HEPES (N-2-hydroyethylpiperazine-N9-2ethanesulfonic acid) [pH 7.9], 60 mM NaCl, 5 mM $MgCl_2$, 1 mM dithiothreitol, 0.5 mM phenylmethylsulfonyl fluoride, 4% glycerol, and 50 µg/ml poly[d(I-C)], before the addition of the radiolabeled probe. For competition assays, binding reactions included a 100-fold excess of unlabeled oligonucleotide containing the NF-κB consensus binding site or a mutated sequence that disrupts binding of NF-κB (5'-AGTTGAGGcGACTTTCCCAGGC-3', NF-κB site underlined and mutated nucleotide in lower case). For supershift experiments, lysates were pre-incubated for 25 minutes with 1 µg of anti-p65 (sc-372 or sc-109) or anti-CREBII (sc-22800X) (all from Santa Cruz Biotechnology) before adding radiolabeled probe. Binding reactions were resolved by electrophoresis at 4ºC on 5% polyacrylamide gels run in 0.25X TBE buffer under non-denaturing conditions. Gels were dried and autoradiographied, and the intensity of the retarded bands was quantified with Metamorph (Molecular Devices, Sunnyvale, California, USA).

Plasmids, siRNAs, transient transfection and dual luciferase activity assay. The vectors pcDNA3.1$^+$-HOXA9 (human), pcDNA3.1$^+$-HOXA2 (human), p65-GFP, 5xNF-κB-luciferase (a luciferase reporter gene containing a tandem arrangement of five NF-κB binding sites) and pGL3-basic human HOXA9 promoter-luciferase were kindly provided by Dr. C. Patel.[3, 4] The plasmid mut IκBα S32/36A vector (a gift from Dr. P. Muñoz-Canoves) encodes an undegradable form of NF-κB inhibitor alpha (IκBα) and thus functions as a super-repressor of NFκB activity. Small interfering RNA against *hoxa9* (*Hoxa9*-siRNA, Inventoried Cat. # 4392420; Id. s6774) and control-siRNA (*Silencer* Select Negative Control No. 1 siRNA; Cat. # 4390843) were purchased from Life Technologies (Carlsbad, California, USA). One day after seeding in 24-well plates, cells were transiently transfected with 0.25, 0.5 or 1.75 µg of total DNA for E19P, mouse SMCs or rat SMCs, respectively, using 1, 4 or 8 µl of Lipofectamine 2000 (Life Technologies) for E19P, mouse SMCs and rat SMCs, respectively. In brief, cells were co-transfected with 0.1, 0.2 or 0.8 µg NF-kB-luciferase or HOXA9 promoter luciferase vectors and 0.02, 0.04 or 0.15 µg pRL-TK Renilla (control for transfection efficiency; Promega, Madison, Wisconsin, USA) for E19P, mouse SMCs or rat SMCs, respectively. When indicated, cells were co-transfected with pcDNA3.1$^+$-HOXA9, pcDNA3.1$^+$-HOXA2, mut IκBα S32/36A or p65-GFP, with the same amount of plasmid than the one used for the corresponding luciferase vectors. When

indicated, cells were also treated with TNFα (10 ng/ml) during the last 4 hours. One day after transfection, cell lysates were prepared and firefly and renilla luciferase activities were measured with the Dual Luciferase Reporter Assay kit (Promega) and a Sirius Single Tube Luminometer (Berthold Detection Systems, Pforzheim, Germany).

For the siRNA studies, E19P cells or mouse TA-SMCs were seeded for 1 day in 60 mm plates and they were transiently transfected with 50 nM siRNA and 5 µl of Lipofectamine 2000.

Flow Cytometry. Cells were detached from the plate 1 day after transfection, with the exception of the cells used to identify STAT5 that were analysed 2 days after transfection. All procedures were performed at room temperature. Cells were fixed with 2% PFA/1% sucrose for 30 minutes and permeabilized with 0,5% triton-X100 for 15 minutes before staining with the specific primary antibodies (1:200 in PBS) for 1 hour. After several washes, cells were incubated with fluorescent secondary antibodies (1:500 in PBS) for 45 minutes. For PE-E-selectin fluorescent labelling, cells were fixed for 30 minutes with 2% PFA/1% sucrose without permeabilization and stained for 30 minutes with PE-E-selectin (1:100 in PBS; BD bioscience). Cells were examined on a LSR Fortessa flow cytometer (BD Biosciences) and data were analyzed with BD FACSDIVA (BD Biosciences) or FlowJo (Inc).

Statistical analysis. Statistical analysis of microarray data is described above. For other experiments, results are expressed as means±SEM, and statistical significance was evaluated by 2-tailed, unpaired Student's *t* test (GraphPad-Prism, GraphPad Software, LaJolla, California, USA). Differences were considered statistically significant at $p<0.05$.

REFERENCES

1. Cheung C, Bernardo AS, Trotter MW, Pedersen RA, Sinha S. Generation of human vascular smooth muscle subtypes provides insight into embryological origin-dependent disease susceptibility. *Nat Biotechnol*. 2012;30:165-173
2. Skalli O, Ropraz P, Trzeciak A, Benzonana G, Gillessen D, Gabbiani G. A monoclonal antibody against alpha-smooth muscle actin: A new probe for smooth muscle differentiation. *J Cell Biol*. 1986;103:2787-2796
3. Trivedi CM, Patel RC, Patel CV. Differential regulation of HOXA9 expression by nuclear factor kappa B (NF-kappaB) and HOXA9. *Gene*. 2008;408:187-195
4. Trivedi CM, Patel RC, Patel CV. Homeobox gene HOXA9 inhibits nuclear factor-kappa B dependent activation of endothelium. *Atherosclerosis*. 2007;195:e50-60